Quantification of Allosteric Influence of *Escherichia coli* Phosphofructokinase by Frequency Domain Fluorescence

Audrey S. Pham* and Gregory D. Reinhart†
*Division of Pathology and Laboratory Medicine, The University of Texas M. D. Anderson Cancer Center, Houston, Texas 77030; and †Department of Biochemistry and Biophysics, Texas A&M University, College Station, Texas 77843

ABSTRACT The allosteric properties of the wild-type *Escherichia coli* phosphofructokinase were compared to the E187A mutant by using frequency-domain techniques. Tryptophan-shifted mutants comprising of double (W311Y/Y55W and W/311F/F188W) and triple (W311Y/Y55W/E187A and W311F/F188W/E187A) amino acid residue changes, which allowed for better fluorescence probing at targeted sites, were also compared to the wild-type and E187A. The additive nature of multiple mutations allowed one to partition the net effect of modifying residue 187. In general, the mutant enzymes displayed greater heterogeneity in sub-state population than did the wild-type enzyme. The semi-cone angle model was used to quantify the extent of depolarization of the fluorophore. Use of the model presupposes that the extent of depolarization directly correlates with the degree of flexibility of the fluorophore. A relationship has been established between the values determined from the semi-cone angle calculations and the thermodynamic components responsible for the allosteric linkage between the regulatory and substrate binding. Coupling interactions giving rise to positive entropy components are manifested by increasing flexibility of the ternary complexes rather than the binary complexes.

INTRODUCTION

The primary strategy of *Escherichia coli* phosphofructokinase (PFK) regulation is for a single inhibitor phosphoenolpyruvate (PEP) or activator MgADP to bind to an alternative (allosteric) site and influence the affinity of substrates toward the enzyme. In the wild-type enzyme, MgADP binding to a regulatory site increases, whereas PEP decreases, the binding affinity of Fru-6P to the active site (Blangy et al., 1968). The glutamate at position 187 of each of the homologous tetrameric subunits presumably plays a crucial role in either the binding of effector ligands to the regulatory site (Shirakihara and Evans, 1988) or the changing of substrate binding affinity to the enzyme (Lau and Fersht, 1987, 1989; Auzat et al., 1994). The allosteric properties with respect to the E187A mutant have been thoroughly examined using steady-state kinetics, transient kinetics, and steady-state fluorescence (Lau and Fersht, 1987, 1989; Auzat et al., 1994; Pham et al., 2001; Pham and Reinhart, 2001a,b).

In the E187A mutant, MgADP loses its activating effects toward the binding affinity of Fru-6P even though MgADP binds to the mutant with comparable affinity as with the wild-type enzyme (Pham et al., 2001). Pre-steady-state kinetics data indicate that linkage between MgADP and Fru-6P persists, even in the absence of allosteric effects (Pham, 1999). Linkage is defined as the reciprocity of influences exerted among multiple ligands binding mutually to an enzyme. If ligand X increases the affinity of A to the enzyme, then A is said to exert the same influence on X. For the E187A mutant, the interaction of Fru-6P and MgADP to PFK gives rise to a net coupling free energy of zero. By using dynamic fluorescence techniques, the coupling free energy of Fru-6P and MgADP binding can be partitioned into its components to determine whether the net coupling free energy results from a reciprocal cancellation of the energetic components (linkage) or from the absence of ligand interaction (no linkage).

The E187A mutation causes PEP, a wild-type inhibitor of Fru-6P binding, to enhance substrate binding only when the co-substrate MgATP is present above a threshold amount. PEP weakly inhibits the binding of Fru-6P to the enzyme at concentrations of MgATP <25 μM (Pham and Reinhart, 2001a). Crossover from activation to inhibition occurs at a concentration of ~ 25 μM. Stopped-flow kinetics results indicate that the allosteric activity for the wild-type *E. coli* PFK occurs by modifying existing rate constants, rather than introducing additional processes (Pham and Reinhart, 2001b). Indeed, weak allosteric influence in the E187A mutation occurs by decreasing the magnitude of rate and equilibrium constants while preserving the basic two-step process of binding. In this report, we sought to investigate how these activation and inhibition phenomena are manifested on the timescale of dynamic fluorescence lifetimes.

The advantage of utilizing a single fluorophore probe is that a significant fraction of the fluorescence signals supposedly reflect the environmental dynamics concentrated within the vicinity of the fluorophore. Tryptophan-shifted mutagenesis strategy was employed to relocate the intrinsic fluorophore closer to the allosteric binding site. The tryptophan residue at position 311 was substituted with either a phenylalanine or tyrosine. Conversely, the reciprocal phenylalanine or tyrosine, formerly located within the vicinity of the regulatory binding site, was substituted with a tryptophan. The result was a double mutation in which the

Submitted June 18, 2002, and accepted for publication January 13, 2003.
Address reprint requests to Audrey S. Pham, 1515 Holcombe Boulevard, Box 84, Houston, TX 77030-4009. Tel.: 713-792-0729; Fax: 713-792-0936; E-mail: aspham@mail.mdanderson.org.

0006-3495/03/07/656/11 $2.00

tryptophanyl fluorophore was effectively relocated to the site more useful for probing ligand binding to the allosteric site. The tryptophan-shifted strategy preserves the amino acid makeup because the residues merely exchanged positions. Similarity in the backbone structures makes substituting a tryptophan with a tyrosine or phenylalanine a relatively modest alteration to protein structural integrity. Therefore, the change does not significantly affect the functional properties of PFK (Pham, 1999).

An additional E187A mutation was then introduced to the tryptophan-shifted double mutant. Using steady-state kinetics, fluorescence emission, and fluorescence, we have shown that the resultant double and triple mutants are highly sensitive fluorescence probes to monitor ligand binding events (Pham, 1999). In addition, tryptophan-shifted mutants generated at position-55 (W311Y/Y55W and W311Y/Y55W/E187A) have been determined to have additive effects, i.e., the effects attributable to each mutation can be partitioned (Pham, 1999). Changes in the fluorescence properties attributed to the E187A mutation can be determined by canceling effects attributed to other mutations. Alternatively, tryptophan-shifted mutants generated at position 188 (W311F/F188W and W311F/F188W/E187A) have been determined to be synergistic (Pham, 1999). As in this case of neighboring residues 187 and 188, the synergistic characteristic is common when multiple mutations are located close to one another (Wells, 1990). Isolated events at the targeted allosteric site can be monitored by using frequency domain anisotropy.

MATERIALS AND METHODS

Materials

All reagents used were of analytical grade and purchased from either Sigma Chemical (St. Louis, MO) or Fisher Scientific (Pittsburgh, PA). All buffers and stock ligand concentrations were filtered through 0.22-μm membranes obtained from Millipore (Bedford, MA).

Mutation of pfk gene and purification of PFK

The mutations E187A, W311Y/Y55W, W311F/F188W, and W311F/F188W/E187A were generated using the pALTER-1 strategy described previously (Pham et al., 2001). The W311Y/Y55W/E187A mutation was generated using a PCR-based Quik-Change method from Stratagene (Cambridge, United Kingdom). The purification protocol was as previously described (Pham et al., 2001).

Tryptophanyl fluorescence lifetime determination

The harmonic domain method of lifetime determination using cross-correlation frequency was performed as described elsewhere (Spencer and Weber, 1969; Gratton and Limkeman, 1983; Lakowicz and Gryczynski, 1991). In summary, lifetimes were measured using the ISS K2, using the 300-nm line of a Spectra-Physics Model 2045 argon ion laser (Mountain View, CA) as an excitation source. A Pockel cell served as the light modulator, and emissions were collected through a WG-345 filter. Modulation frequencies were generated by a Marconi 2022A frequency synthesizer (London). Cross-correlation was achieved by locking the second frequency synthesizer, which modulated the voltage applied to the photocathode of the photomultiplier tube, in phase with the first synthesizer but at a frequency 80-Hz lower. Consequently, the photomultipliers responded to the low frequency range with an increased signal-to-noise ratio while preserving the phase difference and modulation characteristics of the original high-MHz frequency range. The rotational diffusion biases on the observed lifetimes were eliminated by orienting the emission polarizer at an angle 55° from the vertical laboratory axis (Spencer and Weber, 1969).

The responses of the photomultiplier tubes were inherently biased because of the time-response dependence of photons of different wavelengths impinging on the photo-cathode (Lakowicz et al., 1981). To eliminate this effect, a solution of ρ-terphenyl (Kodak) in absolute alcohol was used to provide a phase and modulation reference that could be measured at the same wavelength as the sample observation (Lakowicz et al., 1981). The assigned lifetime value for ρ-terphenyl is 1.05 ns. As a control, the lifetime determination of *n*-acetyl-tryptophan-amide in phosphate buffer (pH 7/KOH) was determined at the start of each day's operation, after sufficient warmup time, to ensure that no anomalous fluctuation of the instruments occurred. An average lifetime value of ~2.9 ns with a reduced χ^2 close to 1 was usually obtained. Measurements were performed in a 1-cm × 1-cm cuvette with continuous stirring to minimize sample photobleaching. The PFK subunit concentration was ~5 μM for each preparation.

The frequency dependence of the phase and modulation of the tryptophan fluorescence for each unbound and bound enzyme form was determined at 12 or 15 different modulation frequencies, which varied logarithmically from 2 to 250 MHz. Data were collected at each frequency until the standard deviations for each measurement of phase and modulation were below 0.2° and 0.004, respectively. When measuring the lifetimes of the multiliganded complexes, saturating amounts of each ligand of at least 10× above the dissociation constant were added to ensure that a significant fraction of the species existed in binary or ternary complexes. Nitrogen was infused into the sample compartment to prevent condensation on the cuvette when experiments were performed at 5°C. Data were fit to various models, providing for a combination of discrete exponential sums (Jameson et al., 1984) or continuous distribution (Alcala et al., 1987a,b) to describe the total lifetime component(s).

Fluorophore lifetime data analysis

The general law to describe lifetime decay is given by Alcala et al. (1987a), Lakowicz et al. (1984), and Johnson (1997):

$$I_{(t)} = \sum_{i=1}^{N} P_{(\tau)i} e^{(-t/\tau_i)}, \tag{1}$$

where each species contributes to the emission intensity $I_{(t)}$ by a probability distribution function ($P_{(\tau)}$) for nonexponential decay, at time t, and for decay time τ_i of that component. Common functional lifetime distributions such as the Lorentzian, uniform, and Gaussian forms (Alcala et al., 1987a; Johnson, 1997) as well as single and multiple discrete exponentials were all sampled in determining the best fit for the data. The probability distribution function used to describe a Gaussian distribution is given by Johnson (1997):

$$P_\tau = \frac{1}{\sigma_T (2\pi)^{0.5}} e^{-0.5((\tau-\tau_{ave})/\sigma_T)^2}, \tag{2}$$

where τ_{ave} is the mean Gaussian distribution of lifetimes. The standard deviation is described by (σ_T) and the half-width is equal to $2.354\sigma_T$.

Dynamic anisotropy determination

Frequency domain anisotropy was measured by exciting the sample with the amplitude-modulated light polarized vertically (conventional arrangement

described in Pham, 1999). The parallel components were measured by placing the emission polarizers in the vertical position, and the perpendicular components were measured by rotating the emission polarizer to the horizontal position. Eq. 3 was applied to recover the parameters from the anisotropic data and to give rise to individual polarized decays (Lakowicz and Gryczynski, 1991):

$$S_j = \int_o^\infty I_{j(t)} \sin \omega t \, dt \quad \text{or} \quad C_j = \int_o^\infty I_{j(t)} \cos \omega t \, dt. \qquad (3)$$

The value j represents an orientation that can be either a parallel or perpendicular component. The anisotropy value is determined from:

$$r_{(t)} = \frac{\Delta_\omega - 1}{\Delta_\omega + 2} \quad \text{or} \quad r_{(t)} = \frac{\Lambda_\omega - 1}{\Lambda_\omega + 2}, \qquad (4)$$

where

$$\Delta_\omega = \tan^{-1}\left(\frac{C_\parallel S_\perp - C_\perp S_\parallel}{S_\parallel S_\perp + C_\parallel C_\perp}\right) \quad \text{or} \quad \Lambda_\omega = \left(\frac{C_\parallel^2 + S_\parallel^2}{C_\perp^2 + S_\perp^2}\right)^{0.5}. \qquad (5)$$

The $r_{(t)}$ anisotropy can account for multiple fluorophores, when each gives rise to a single rotational correlation time and undergoes unhindered rotations. However, the aromatic intrinsic fluorophore is normally embedded in the protein structure, where movement is somewhat restricted and the angular range of rotational motion attributable to the fluorophore is limited relative to the motion of the protein. In this hindered environment, the anisotropy decay does not extend to zero but rather to a certain plateau value. This motion can be distinguished from the free tumbling motion of the protein by the expression (Munro et al., 1979; Lipari and Szabo, 1980):

$$r_{(t)} = (r_o - r_\infty)e^{-t/\phi_1} + (r_\infty)e^{-t/\phi_2}, \qquad (6)$$

where r_o is the anisotropy that would be observed in the absence of rotational diffusion, i.e., at $t = 0$. The $(r_o - r_\infty)$ term describes the limited rotation experienced by the fluorophore and the term r_∞ describes the overall rotation commonly attributed to protein. Due to the slow tumbling of the macromolecule, the limiting anisotropy (r_∞) often is relatively long compared with the rotational correlation time of the fluorophore, thus allowing for discrimination between the two motions. One motion, ϕ_2, describes the rotational correlation time of the protein. The other motion, ϕ_1, is a function of the rotational diffusion constant limited by some angular range within the semi-cone. This restricted angular range of motion, commonly described as the ''semi-cone angle'' of rotation (Φ) (Munro et al., 1979; Lipari and Szabo, 1980), is determined by the expression (Gratton et al., 1986; Lipari and Szabo, 1980; Munro et al., 1979):

$$\cos(\Phi) = \frac{1}{2}\left\{\left[\left(1 + 3\left(\frac{r_\infty}{r_o}\right)^{1/2}\right)^{1/2}\right] - 1\right\}. \qquad (7)$$

Data analysis

The goodness of fit for each model was determined by inspection of the residuals [$(\delta_\omega - \delta_{c\omega})$ and $(M_\omega - M_{c\omega})$] and by analysis of the reduced $\chi^2(\chi_R^2)$ values (Lakowicz et al., 1984; Gratton et al., 1984):

$$\chi_R^2 = \left(\frac{1}{2N - P}\right)\left[\sum_\omega \frac{1}{\sigma_{\delta\omega}^2}(\delta_\omega - \delta_{c\omega})^2 + \sum_\omega \frac{1}{\sigma_{M\omega}^2}(M_\omega - M_{c\omega})^2\right], \qquad (8)$$

where $\sigma_{\delta\omega}$ and $\sigma_{M\omega}$ are the estimated uncertainties in the phase and modulation, respectively. δ_ω and $\delta_{c\omega}$ are the experimentally determined and predicted (calculated) phase values based on an assumed decay law, respectively. Likewise, M_ω and $M_{c\omega}$ are the measured and predicted modulation values. For error analysis of anisotropy decays, the terms $(\delta_\omega - \delta_{c\omega})$ and $(M_\omega - M_{c\omega})$ are replaced with $(\Delta_\omega - \Delta_{c\omega})$ and $(\Lambda_\omega - \Lambda_{c\omega})$, respectively. Minimization of the χ^2 with respect to α and τ is done by the Marquardt-Levenberg algorithm (Marquardt, 1963). Initial parameter guesses for α and τ were specified at the start of each search. N is the number of frequencies, P is the number of floating parameters, and $(1/(2N-P))$ is the number of degrees of freedom. The uncertainties used in the calculations were $\sigma_{\delta\omega} = 0.2°$ and $\sigma_{M\omega} = 0.004$. The reduced χ^2 and inspection of the residuals were the criteria for determining the best fit model for describing the data.

Data were generally analyzed using GLOBALS Unlimited (Laboratory for Fluorescence Dynamics at the University of Illinois at Urbana-Champaign; see also Knutson, 1992; Beechem et al., 1991). The software allows for simultaneous analyses of multiple data sets by linking certain variables that are considered independent to the experimental condition. This approach simplified our data interpretation because only the trends of one or few pertinent parameters are examined. It must be emphasized that the multiparameter linkage fit of data sets is a model, and that the value of χ_R^2 served as the criterion to determine the fitness of the model describing the linkage variables.

RESULTS

Tryptophanyl lifetime for the E187A mutant PFK

Data for each lifetime measurement were fit to various combinations of models providing for discrete exponential sums and for distribution patterns. In most cases, the major lifetime component of the tryptophanyl fluorophore for the E187A mutant enzyme was best described by a Gaussian distribution, with the distribution alone comprising >94% of the total emission. The minor component was best described by a discrete exponential with a lifetime value of ~0.6 ns. Table 1 shows the lifetime values derived from the fit of the phase and modulation as a function of frequency for the E187A mutant in the unliganded and bound forms. The major component of the tryptophanyl lifetime of each bound species ranged from 4.9 to 6.2 ns. In contrast, the major component of the tryptophanyl lifetime for the wild-type enzyme was well described by the sum of two discrete components, the major component comprising >97% of the total intensity. The lifetime value for the unliganded E187A PFK was indistinguishable from that of the wild-type enzyme.

For each lifetime determination, two fitting methods were compared: an independent fit for each data set and a multiparameter linkage allowing for simultaneous analysis of multiple data sets. Linkage of parameters was based on the assumption that those parameters did not contribute to the phenomenological conditions under study. The results obtained using both methods did not differ significantly. Both methods yielded similar χ^2. However, the linkage method provided additional information pertaining to the enzyme-ligand interactions, i.e., that the minor lifetime component and the width of the distribution were not influenced by the ligand binding events (overall $\chi^2 = 1.3$). The linked parameter values of the half-width at half-maximum height (width) were 0.9 ns for the long lifetime

TABLE 1 Lifetime values for the E187A mutant in the presence of ligand(s)

Sample	τ_1	W	F_1	τ_2	χ^2
E187A	5.91 ± 0.02	0.77 ± 0.08	0.99	1.11 ± 0.08	0.41
+Fru-6P	4.96 ± 0.02	0.55 ± 0.10	0.98	0.85 ± 0.07	0.60
+PEP	5.98 ± 0.03	1.13 ± 0.07	0.99	0.55 ± 0.08	0.84
+$MgADP_{(eff)}$	6.14 ± 0.03	1.53 ± 0.05	0.97	0.47 ± 0.02	0.73
+$MgADP_{(act)}$	6.28 ± 0.02	1.24 ± 0.05	0.99	0.54 ± 0.04	0.37
+Fru-6P, PEP	5.31 ± 0.03	0.91 ± 0.07	0.97	0.60 ± 0.02	0.74
+Fru-6P,$MgADP_{(eff)}$	4.76 ± 0.02	0.98 ± 0.05	0.97	0.48 ± 0.03	0.86
+Fru-6P,$MgADP_{(act)}$	5.15 ± 0.03	1.55 ± 0.03	0.94	0.26 ± 0.01	0.61
+Fru-6P-PEP-ADP	6.23 ± 0.02	1.21 ± 0.06	0.98	0.66 ± 0.04	0.51
+F6P-AMPPCP-PEP	6.09 ± 0.04	2.23 ± 0.09	0.94	0.30 ± 0.01	1.04
+F6P-AMPPCP	4.85 ± 0.03	1.85 ± 0.04	0.95	0.23 ± 0.02	1.25
+PEP-AMPPCP	6.37 ± 0.05	2.30 ± 0.06	0.98	0.26 ± 0.04	2.31
+AMPPCP	6.03 ± 0.04	1.70 ± 0.06	0.96	0.35 ± 0.02	1.26

component and 0.73 ns for the short lifetime component. Fig. 1 shows the distributional patterns for the E187A mutant PFK in the unbound and singly bound forms obtained from the global linkage method. The E187A mutation appeared generally to increase the distribution width. However, the widths of the structures do not differ significantly among the various bound forms of the mutant. Rather, ligand binding appeared to shift the distribution. Fru-6P binding to the E187A mutant produced the most drastic lifetime distributional shift toward a shorter lifetime, whereas MgADP produced a minor shift to a longer lifetime.

To determine whether the observed distributional patterns was due to increased heterogeneity of the environment surrounding the fluorophore, lifetimes determined at 25°C were compared with those at 5° and 35°C. Structural heterogeneity manifests by changes in the width structures at different temperatures. Increasing the temperature would presumably cause an increase in the rate of substates interconversion sampled by the fluorophore. If the increased rate of interconversion is greater than the lifetimes of the fluorophore, then the environment of the fluorophore appeared to be more homogeneous. The size of the distribution width, then, would be temperature-dependent. However, this was not the case since the distribution width was wider at the two extremes of temperature (data not shown). These trends were observed for all enzyme species. Generally, the types of changes observed most evident are the distributional shifts. Fru-6P binding caused a shift to a shorter lifetime whereas PEP and MgADP caused shifts to longer lifetimes.

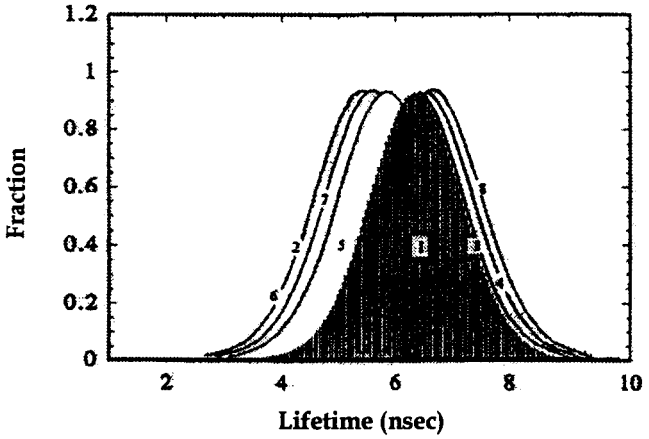

FIGURE 1 Fluorescence lifetime distribution patterns for the E187A mutant phosphofructokinase. The profiles shown are in the unbound protein (*1*) and protein in the presence of 5 mM Fru-6P (*2*); 10 mM PEP (*3*); 0.2 mM MgADP (*4*); Fru-6P + PEP (*5*); Fru-6P + MgADP (*6*); 3 mM MgADP (*7*); and Fru-6P + MgADP (*8*). The patterns represent the results of fitting to a continuous Gaussian distribution for the major component and a discrete lifetime for the minor component (not shown). Results were from global analysis in which the distributional width and minor component were linked.

Dynamic anisotropy measurements of the E187A

The local movement of a probe can be distinguished from the global tumbling of the macromolecule by differential anisotropy. An inherent presumption of this approach is that the overall protein molecule rotates on a much longer timescale than a localized single amino acid fluorophore. Anisotropic measurements were made under the same conditions as those of the lifetime determinations. Data were fit to various models ranging from a sum of discrete exponentials, which describes unhindered and isotropic movements to hindered motion, in which the motion of the fluorophore is restricted (Lakowicz, 1983). Various liganded combinations were sampled for the E187A mutant and the resulting differential phase shifts are shown in Fig. 2. Typically, the differential phase shift showed a wavy curve with the peak magnitude at a frequency that is dependent on the rotational rate, fluorescence lifetime, and limiting anisotropy value (Jameson and Hazlett, 1991). The phase peak tended to shift toward higher frequency with shorter rotational correlation time. Multiple peaks and shoulders suggested complex systems with multiple correlation times. Some negative phase delays were apparent for several of the bound species.

Data sets were fit to Eq. 6 using the lifetime values given in Table 1, and the results are shown in Table 2. Dynamic anisotropy of ligand binding to the E187A mutant PFK was

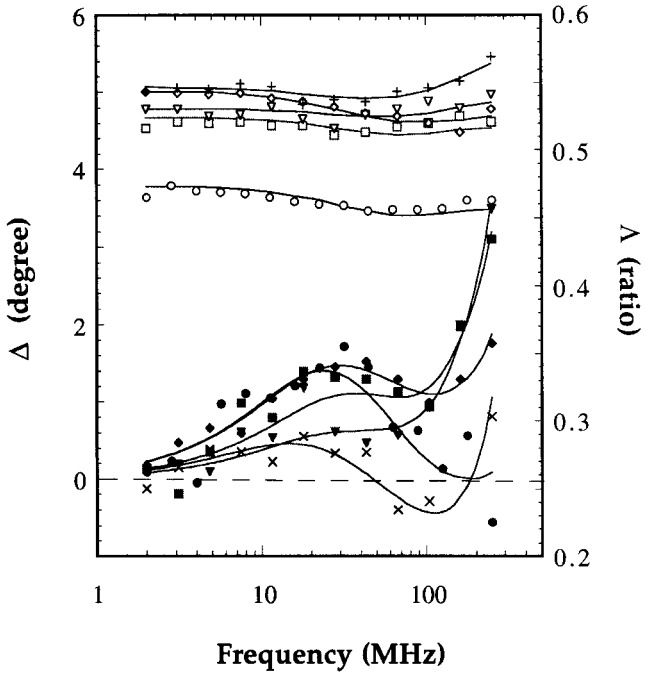

FIGURE 2 Dependence of the anisotropy phase shift (*solid symbols*) and modulation ratio (*unfilled symbols*) as a function of frequency for the E187A mutant phosphofructokinase. Represented here are the unbound PFK (○, ●) and PFK in the presence of 2 mM Fru-6P (■, □); 2 mM F6P and MgADP (▼, ▽); Fru-6P and PEP (◆, ◇); or Fru-6P, PEP and AMPPCP (×, +). The solid lines represent the fitting of data using the cone-angle model described in the text.

best described by the semi-cone angle-of-rotation model, which accounted for a permissible range of movement of a fluorophore side chain about its localized environment. The semi-cone angle reflects the extent of depolarization about a fixed axis. Because the depolarization of the emission transition dipole occurs from an excitation axis, the diffusion event from this reference axis takes on an angular value resembling a half-cone. The χ^2 range indicates the semi-cone angle model adequately characterizes the environment of the fluorophore and the changes associated with the binding of ligand.

Correlation of probe dynamics with thermodynamic properties of coupling interactions

The cone-angle of diffusion values reported here are strikingly consistent with our findings of a positive correlation between the thermodynamic entropy component and the degree of flexibility associated with the tryptophan side chain. The coupling of PEP to Fru-6P in the wild-type enzyme has been shown to be enthalpy-driven, with the absolute value of ΔH greater than the absolute value of ΔS (Johnson and Reinhart, 1997). It can be shown that for an enthalpy-dominated system, an interaction that is inhibiting (ΔG positive) will result in a positive entropy component. Likewise, an enthalpy-dominated interaction that is activating will result in a negative entropy component. The relationship among the energetic components for an enthalpy-dominated reaction is depicted below. The signs in the first row represent an inhibiting interaction (ΔG positive) and the signs in the second row indicate an activating interaction (ΔG negative):

$$\begin{array}{ccccc} \mathbf{\Delta H} & \mathbf{-} & \mathbf{T\Delta S} & = & \Delta G \\ + & & + & & + \\ - & & - & & - \end{array} . \qquad (9)$$

Because the enthalpy and entropy components are compensatory, the magnitude of the contribution is modified accordingly while the signs remain the same. This phenomenon has been consistently observed for the present system under study, for the wild-type *E. coli* PFK and/or couplings interaction in other systems (Braxton et al., 1996; Johnson and Reinhart, 1994; Tlapak-Simmons and Reinhart, 1994)

We have reported that, for the E187A mutant PFK, PEP inhibits Fru-6P when MgATP is absent (Pham and Reinhart, 2001a). This coupling interaction has also been shown to be enthalpy-driven, with the positive contribution of enthalpy being greater than that of entropy. This enthalpy-driven inhibiting interaction of PEP-Fru-6P took on some positive ΔS value (Pham and Reinhart, 2001a). Furthermore, the entropy value reflects the net difference of the competing

TABLE 2 Dynamic fluorescence anisotropy parameters for the E187A mutant of phosphofructokinase

PFK sample	r_o–r_∞	r_∞	ϕ_1	ϕ_2	Φ	χ^2
E187A	0.104	0.296	72 ± 9	0.001	13.4	2.14
+Fru-6P	0.152	0.247	81 ± 19	0.13 ± 0.017	16.8	2.09
+PEP	0.116	0.284	84 ± 12	0.052 ± 0.018	14.3	1.93
+$MgADP_{(eff)}$	0.060	0.287	100 ± 10	0.55 ± 0.06	10.7	0.68
+$MgADP_{(act)}$	0.111	0.288	126 ± 20	0.006 ± 0.015	14.0	1.28
+MgADP, PEP	0.113	0.287	94 ± 16	0.079 ± 0.02	14.1	2.40
+Fru-6P, PEP	0.163	0.236	117 ± 30	0.17 ± 0.016	22.4	1.80
+Fru-6P,$MgADP_{(eff)}$	0.144	0.256	166 ± 70	0.229 ± 0.03	16.2	2.52
+Fru-6P,$MgADP_{(act)}$	0.147	0.236	64 ± 5	0.322 ± 0.016	16.9	0.51
+Fru-6P, AMPPCP	0.142	0.258	62 ± 11	0.286 ± 0.03	16.1	2.68
+Fru-6P, AMPPCP, PEP	0.159	0.228	156 ± 33	0.215 ± 0.02	17.6	0.89
+AMPPCP, PEP	0.111	0.289	92 ± 14	0.07 ± 0.02	13.9	2.57
+AMPPCP	0.115	0.284	103 ± 10	0.311 ± 0.02	14.2	0.44

individual processes in an interaction. While it may be difficult to tease apart these distinct biophysical processes, we can relate macroscopically the net entropy contribution in a disproportionation reaction, reflecting the competing equilibria in a solution:

$$\begin{array}{c}\mathbf{PEP\text{-}PFK} + \mathbf{PFK\text{-}Fru\text{-}6P} \overset{\Delta S>0}{\rightleftharpoons} \mathbf{PEP\text{-}PFK\text{-}Fru\text{-}6P} + \mathbf{PFK} \\ (\mathbf{14}^\circ \pm 0.1) \quad (\mathbf{17}^\circ \pm 0.3) \qquad\qquad (\mathbf{20}^\circ \pm 0.2) \quad (\mathbf{13}^\circ \pm 0.2)\end{array}. \tag{10}$$

The net difference of the ΔS term in this reaction reflects the direction of the equilibrium and therefore the relative magnitude of the ternary coupling interaction. For an enthalpy-driven inhibiting reaction, a positive entropy term may be manifested by increased flexibility on the right side of the equilibrium. Indeed, the summation of the semi-cone angle degree on the right side of the expression is higher than the summation of the degree on the left side of the equation. Furthermore, the modest difference in the degree of flexibility may reflect the weak coupling between Fru-6P and PEP, as was shown using steady-state techniques (Pham and Reinhart, 2001a). Although the difference in these values borders significance, we can conclude qualitatively that the entropy component on the right side of the disproportionation equation, which describes the ternary complex of the reaction, confers relatively more flexibility than either of the bi-liganded species.

Again, the summation on the right side of the equilibrium is relatively higher than the summation of the left side of the equilibrium, indicating a positive correlation between the entropy component and the physical phenomenon. The small net difference in the degrees of semi-cone angles may reflect a weak activating interaction. Thus, regardless of whether the interaction is a result of activation or inhibition, or whether it is entropy- and enthalpy-dominated, the positive entropy term manifested itself by increasing flexibility of the ternary complex than either the bi-liganded species.

The loss by MgADP of its allosteric effects on Fru-6P lead to a coupling free energy of zero, as the coupling constant $Q_{ay} \cong 1$. We have shown that the coupling free energy of zero resulted from a complete and mutual cancellation of some nonzero enthalpy and nonzero entropy contributions, rather than from an absence of MgADP binding or linkage interaction with Fru-6P (Pham et al., 2001). If, as shown previously, the entropy component is instrumental in establishing the magnitude of the coupling interaction, then for a coupling interaction with a free energy of zero, the correlated entropy contribution reflects a net difference of zero:

$$\begin{array}{c}\mathbf{MgADP\text{-}PFK} + \mathbf{PFK\text{-}Fru\text{-}6P} \overset{\Delta S>0}{\rightleftharpoons} \mathbf{MgADP\text{-}PFK\text{-}Fru\text{-}6P} + \mathbf{PFK} \\ (\mathbf{11}^\circ \pm 0.2) \quad (\mathbf{17}^\circ \pm 0.3) \qquad\qquad (\mathbf{16}^\circ \pm 0.2) \quad (\mathbf{13}^\circ \pm 0.2)\end{array}. \tag{13}$$

For an entropy-dominated system, the sign of ΔG is largely dependent on the $T\Delta S$ term:

$$\begin{array}{ccccc}\mathbf{\Delta H} & \mathbf{-} & \mathbf{T\Delta S} & = & \Delta G \\ + & & \mathbf{+} & & \mathbf{-} \\ \mathbf{-} & & \mathbf{-} & & +\end{array}. \tag{11}$$

When two ligands enhance each other's binding in an entropy-driven interaction, the entropy term will also be positive. We have shown previously that activation of Fru-6P by PEP in the presence of MgATP is entropy-driven (Pham and Reinhart, 2001a). Although complications from catalysis precluded us from measuring the Fru-6P-MgATP coupling using fluorescence techniques, we have shown that an ATP analog adenylyl-(β-γ-methylene)-diphosphonate (AMPPCP) also induces PEP to enhance the binding of Fru-6P to roughly the same magnitude as does MgATP (Pham and Reinhart, 2001a,b). The relative difference in the semi-cone angles for the activating interaction of Fru-6P-PEP in the presence of AMPPCP is expressed in the disproportionation equilibrium:

$$\begin{array}{c}\mathbf{PEP\text{-}PFK} + \mathbf{PFK\text{-}Fru\text{-}6P} \overset{\Delta S>0}{\rightleftharpoons} \mathbf{PEP\text{-}PFK\text{-}Fru\text{-}6P} + \mathbf{PFK} \\ \mathbf{AMPPCP} \quad\quad \mathbf{AMPPCP} \qquad\qquad \mathbf{AMPPCP} \quad\quad \mathbf{AMPPCP} \\ (\mathbf{14}^\circ \pm 0.3) \quad (\mathbf{16}^\circ \pm 0.3) \qquad\qquad (\mathbf{14}^\circ \pm 0.4) \quad (\mathbf{18}^\circ \pm 0.3)\end{array}. \tag{12}$$

Characterization of tryptophan-shifted mutant lifetimes

The lifetime parameters for the double mutants (DM) and triple mutants (TM) generally exhibited considerable heterogeneity, giving rise to wider distributional widths and greater lifetime changes upon ligand binding. Fig. 3 compares the frequency dependence of phase and demodulation for the wild-type, E187A mutant, and tryptophan-shifted mutant enzymes. Each enzyme species exhibited distinct phase and modulation patterns, even though few differences were observed among the species from steady-state kinetics and fluorescence techniques. One of the signatures of heterogeneous lifetimes is the incomplete phase lag, giving rise to a depressed segment in the high frequency range. These trends suggested that the tryptophan-shifted mutations, which located the fluorophore closer to the solvent surface, increased the heterogeneity of the environment surrounding the fluorophore. Again, the global-linkage model did not

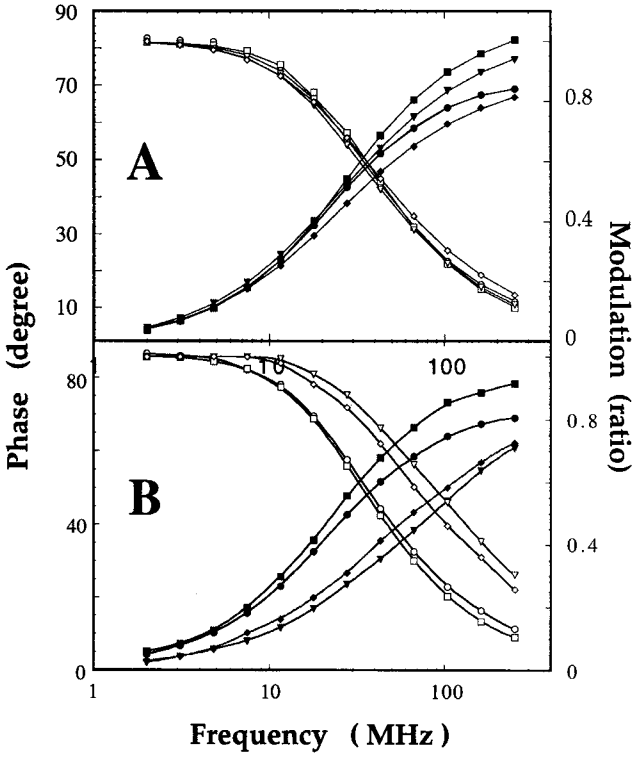

FIGURE 3 Dependence of the phase shift and modulation ratio as a function of frequency for tryptophan-shifted phosphofructokinase mutants. Measurements were performed by exciting the tryptophanyl fluorophore at 300 nm and collecting emission frequencies of 3–250 MHz. Solid symbols correspond to the phase shift, and unfilled symbols correspond to the modulation ratio. (*A*) Comparison of the phase and modulation changes for the free enzyme forms of the wild-type (●, ○), E187A (■, □), W311Y/Y55W (▼, ▽), and W311Y/Y55W/E187A (◆, ◇). (*B*) Comparison of the phase and modulation changes for the free enzyme forms of the wild-type (●, ○), E187A (■, □), W311F/F188W (▼, ▽), and W311F/F188W/E187A (◆, ◇).

describe the dynamic characteristics of the tryptophan-shifted mutants well; all linked combinations yielded higher χ^2 values. Tables 3 and 4 summarize the results, from each independent fit to a Gaussian distribution and a minor discrete exponential, for the position-55 tryptophan-shifted mutants. For all of the tryptophan-shifted mutants, the width of the Gaussian distribution was increased significantly. The average lifetime values for the DM55 and TM55 mutants were comparable to those for the wild-type and the E187A mutant enzymes, with a median distribution of ~6 ns. In the absence of any ligands, the proteins behaved identically. Lifetime values were shown to be ~6 ns, half-width distributions were ~2.82, and the majority of the fraction occupied the distribution pattern, with <5% displaying a discrete lifetime. In most cases, the presence of effector ligands reduced the lifetimes, with Fru-6P and MgADP causing decreases that are even more drastic. Ligands binding to the allosteric site caused a wider distribution than ligands binding to the active site.

Changes in the lifetime values upon ligand binding were similar for the single mutant E187A and the TM55 mutant, both of which incorporated the Glu-to-Ala mutation, but change was not as drastic as for the DM55 mutant. Like the position-55 mutants, the tryptophan-shifted position 188 mutants displayed considerable heterogeneity (Fig. 3). However, the changes in the lifetime values for these mutants did not reflect lifetime characteristics that could be easily interpreted. For example, some of the bound species were best described by a Lorentzian distribution, and others by a Gaussian form (data not shown). Steady-state measurements revealed that the effects of the position-188 mutations were synergistic (Pham, 1999). Therefore, we cannot extract, even qualitatively, the net effect of the E187A mutation from the DM188 and TM188.

Dynamic anisotropy characterization of the tryptophan shifted mutants

The correlation of the entropy term to the flexibility of the tryptophan side chain of the E187A mutant was arguably inconclusive due to the small net difference in the reported values. As an attempt to augment these differences in the cone angles, we shifted the tryptophan residue, which is unique to the protein, to the targeted site to effect fluorescence probing in this localized region. The assumption was

TABLE 3 Fluorescence lifetime parameters for the W311Y/Y55W mutant of phosphofructokinase

PFK sample	τ_1	W	F_1	τ_2	χ^2
W311Y/Y55W	6.63 ± 0.03	2.98 ± 0.03	0.95	4.55 ± 0.39	0.68
+Fru-6P	2.10 ± 0.04	1.07 ± 0.08	0.50	1.07 ± 0.02	1.25
+PEP	5.08 ± 0.02	1.40 ± 0.03	0.97	0.38 ± 0.02	0.57
+$MgADP_{(eff)}$	1.04 ± 0.11	5.29 ± 0.07	0.92	0.35 ± 0.02	1.25
+$MgADP_{(act)}$	2.18 ± 0.08	4.71 ± 0.04	0.96	0.48 ± 0.05	1.95
+Fru-6P, PEP	5.38 ± 0.13	5.95 ± 0.15	0.54	5.35 ± 0.10	1.99
+Fru-6P,$MgADP_{(eff)}$	1.48 ± 0.11	2.10 ± 0.12	0.43	1.24 ± 0.02	2.28
+Fru-6P,$MgADP_{(act)}$	0.57 ± 0.10	2.70 ± 0.67	0.47	1.23 ± 0.02	1.29
+PEP, MgADP	2.20 ± 0.19	4.71 ± 0.17	0.94	0.35 ± 0.06	3.82
+Fru-6P, AMPPCP	3.85 ± 0.06	4.48 ± 0.09	0.95	1.75 ± 0.16	1.42
+Fru-6P, AMPPCP, PEP	3.85 ± 0.04	2.57 ± 0.08	0.99	0.02 ± 0.01	1.89
+AMPPCP, PEP	4.66 ± 0.06	4.22 ± 0.10	0.94	1.49 ± 0.2	1.28
+AMPPCP	5.43 ± 0.07	3.22 ± 0.11	0.97	0.34 ± 0.05	3.33

TABLE 4 Fluorescence lifetime parameters for the W311Y/Y55W/E187A mutant of phosphofructokinase

PFK sample	τ_1	W	F_1	τ_2	χ^2
W311Y/Y55W/E187A	5.80 ± 0.02	2.82 ± 0.05	0.99	0.22 ± 0.16	1.06
+Fru-6P	5.41 ± 0.09	3.06 ± 0.17	0.92	2.72 ± 0.47	0.66
+PEP	1.80 ± 0.14	4.78 ± 0.04	0.52	4.52 ± 0.08	1.61
+$MgADP_{(eff)}$	5.90 ± 0.03	3.54 ± 0.06	0.96	0.31 ± 0.02	0.49
+$MgADP_{(act)}$	5.19 ± 0.14	4.29 ± 0.22	0.91	0.26 ± 0.03	5.34
+Fru-6P, PEP	4.41 ± 0.02	1.81 ± 0.02	0.97	0.16 ± 0.03	0.51
+Fru-6P,$MgADP_{(eff)}$	3.66 ± 0.05	3.35 ± 0.11	0.85	2.39 ± 0.10	1.61
+Fru-6P,$MgADP_{(act)}$	5.43 ± 0.11	3.82 ± 0.21	0.90	0.34 ± 0.02	4.47
+PEP, MgADP	4.92 ± 0.08	2.72 ± 0.14	0.90	0.29 ± 0,02	3.80
+Fru-6P, AMPPCP	4.88 ± 0.09	5.63 ± 0.13	0.99	0.27 ± 0.19	1.79
+Fru-6P, AMPPCP, PEP	3.33 ± 0.03	2.38 ± 0.05	0.97	15.1 ± 1.0	2.09
				1.61 ± 0.06	
+AMPPCP, PEP	4.44 ± 0.02	2.70 ± 0.03	0.89	20.9 ± 1.3	0.62
				0.07 ± 0.05	
+AMPPCP	5.12 ± 0.02	2.68 ± 0.01	0.81	11.6 ± 0.46	0.88
				0.05 ± 0.03	

that the tryptophan shift would heighten sensitivity and amplify the net difference of the entropy terms. Because steady-state measurements have revealed that mutation-induced changes to position-55 double and triple mutants are additive in nature, the net effects of the E187A mutation can be quantified (Pham, 1999). Anisotropy phase difference and modulation were measured for both of the DM55 and TM55 mutants. Fig. 4 shows the dependence of these phase difference and modulation ratios on frequency for the DM55 and TM55 mutants. Introducing the probe near the allosteric site did enhance the anisotropy contribution, as evidenced by the increased (at least twofold) amplitudes of the phase difference from either the wild-type enzyme or the E187A mutant. However, the structure that contributed most significantly to the anisotropy characteristic was shifted toward a higher frequency range. Although this shift suggested a decrease in rotational correlation time associated with faster motion, the shift was also toward the limit of the detection system. Thus, the rising segment in the high frequency range, which reflected a significant proportion of the total anisotropy decay, presented an uncertainty in the amplitude limit and the extent of the structure. Consequently, not all of the data sets could be analyzed. Partial results are presented in Table 4. A similar increase in the phase difference was also noted for the E187A mutant. However, significant anisotropy components were also evident in the lower frequency range, allowing for the reasonable fitting of data.

DISCUSSION

The spectral characteristics of a tryptophan in a protein may vary widely due to the flexibility of the side chain and its exposure to a wide range of environments. In the present study, we sampled dynamic fluorescence of the *E. coli* PFK by placing the tryptophanyl probe in three different environments: the original position-311 in the hydrophobic region of the protein, the position 55 where the replaced tyrosine was thought to flip-flop in solution when the protein is unbound (Daugherty et al., 1991), and the position-188 where the phenylalanine was next to the pivotal 187 Glu-to-

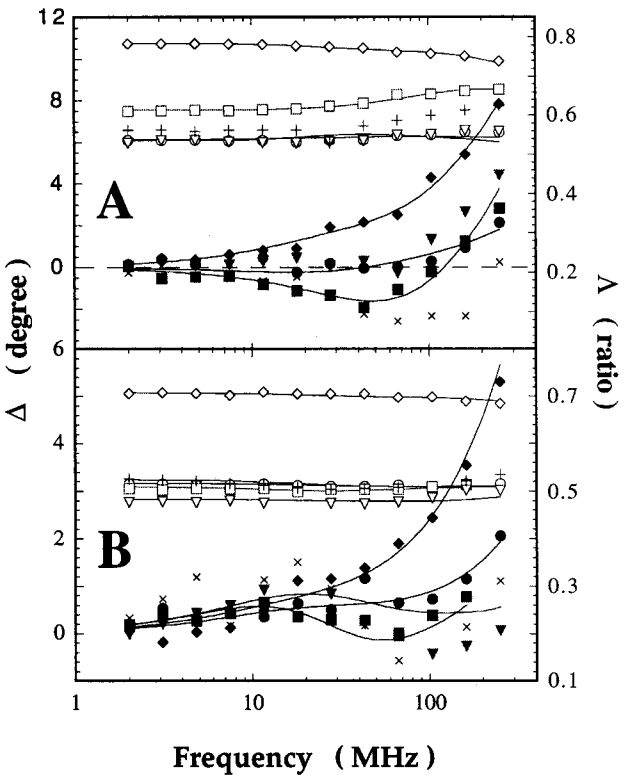

FIGURE 4 Dependence of the anisotropy phase shift (*solid symbols*) and modulation ratio (*unfilled symbols*) as a function of frequency for the position 55 tryptophan-shifted phosphofructokinase mutants. Shown are the results for W311Y/Y55W (*A*) and the W311Y/Y55W/E187A (*B*) in the unbound state (●, ○), and in the presence of saturating amount of Fru-6P (■, □); Fru-6P and MgADP (▼, ▽); Fru-6P and PEP (◆, ◇); and Fru-6P, PEP and AMPPCP (×, +). The solid lines represent the fitting of data using the cone-angle model described in the text.

Ala mutant. The fluorescence lifetimes of the probe in the three different positions were considerably heterogeneous. In most cases, the tryptophanyl lifetime was well-described by a Gaussian distribution for the major component and a single exponential for the shorter lifetime component.

Heterogeneity arises from a fluorophore when it is undergoing excited state reactions, such as exciplex formation, solvent relaxation, proton transfer, and energy transfer, in addition to configuration changes (Gratton et al., 1984; Munro et al., 1979; Ansari et al., 1985; Valeur and Weber, 1977). It may also arise from tryptophan having overlapping ^1L_a and ^1L_b differentially-polarized electron transitions. The ^1L_a is thought to be more sensitive to environmental perturbations than the ^1L_b transition (Platt, 1951). Indoles have been found to form both excited-state and ground-state complexes with polar compounds, resulting in shifts of the absorption/emission spectra and multiple fluorescence lifetimes (Callis, 1999).

Lifetime distribution is dependent on the environment of the fluorophore (Alcala et al., 1987). Possible factors accounting for complex decays coming from a single fluorophore are differences in microenvironments, the existence of multiple conformations, excited-state reactions such as exciplex formation, excited-state solvent relaxation, *cis-trans* isomerization, or excited-state proton transfer energy transfer. Differences in substates may be due to shifting of bonds, rotation of side chains, or displacement of secondary features. Emission decay properties are a function of flexibility of the fluorescent probe, the microheterogeneity of the probe's environment, and the rate of interconversion. Our interpretation of these decays relies on the assumption that the decay values correspond to the conformations or subconformations. The lifetime distribution arises from a possibility of either the fluorophore being responsive to the different environments or the rate of the probe interconversion being slower than excited-state lifetime. Sometimes, when the rate of conversion is extremely fast relative to its lifetime, an apparent single average environment is detected. Of course, other phenomena can also cause the heterogeneous distribution of decay rates; these include the energy transfer between the acceptor and the donor (Haran et al., 1992) and the characteristics of the quencher.

The width of the lifetime is associated with the heterogeneity of the sample. A narrow lifetime distribution may indicate either a homogenous system or even a heterogeneous system with very fast dynamics. These possibilities can be discriminated by either altering a parameter that can affect the dynamics of the system (e.g., temperature or viscosity), or measuring the decay of the differential anisotropy. Our temperature studies did not yield straightforward interpretations of the distributional width. The Gaussian distribution may reflect, on the one hand, a distribution of microstates representing a sharing of the energy-minima well or, on the other hand, multiple exponential decays that are too close together on a timescale to be resolved. When transitions between substates occur more slowly, then the decay distributional patterns are evident. This, in turn, represents the existence of several macrostates that may be due to the various bound states available to the protein.

Factors underlying the lifetime distribution may be static or dynamic (Demchenko, 1994). A continuum of conformational substates would each have its own lifetime and thus constitute a static cause of the distribution decay. However, collisional interaction of the fluorophore with the surrounding molecules, which consists of an array of amino acid residues, may result in dynamic quenching. One or both of these processes may occur and can be discriminated through temperature or viscogen studies. Our results for the E187A mutant suggest that the distributional decay may be static in nature, since the width of the distribution was not substantially affected by changes in temperatures. In addition, global linkage of multiparameter data sets suggests that the distributional width is not influenced by the ligation state of the protein. Perhaps performing dynamic anisotropy at several different excitation wavelengths may also provide additional information about the collision activity of the molecule, since excitation at different wavelengths can affect the orientation of the absorption dipoles (Lakowicz and Gryczynski, 1991).

The negative phase delay we observed was probably caused by an association between the multiple decay times and the individual correlation times (Jameson and Sawyer, 1995, Szmacinski et al., 1987). Although this phenomenon has been reported for multiple emitting species with distinct lifetime values and rotational correlation times (Szmacinski et al., 1987; Knutson et al., 1986), we observed an associative decay of a single emitting species whose distributional lifetime components conferred two distinct rotational correlation times. Apparent from the phase shift difference is the appearance of a second wavy curve toward the higher frequency range (Fig. 3). Although technical limitations preclude the elucidation of these structures, we can make two qualitative conjectures. First, the appearance of structures in the high frequency range indicates the existence of short rotational components. Second, the substantial amplitude of these structures suggests a significant contribution to the total anisotropic decay.

In conclusion, we have reported here positive correlations between the dynamic and quantitative thermodynamic properties of several coupling interactions involving *E. coli* PFK. The positive correlations lend support to the claim that a coupling free energy may reflect a state in which enthalpy and entropy components compensate for each other. The net differences in the entropy term of the disproportionation equilibria are small, which may reflect cancellations of components rather than lack of interactions. Perhaps there exist correlations between the entropy component and semicone angles of diffusion in the tryptophan-shifted DM55 and TM55 mutants, but we cannot ascertain the relationship until these mutants can be characterized using an instrument that

allows for intensity modulation and detection beyond the 250 MHz range. In addition, due to the associated high errors, it is difficult to interpret the short lifetime component commonly found for all species of *E. coli*. Our 250-MHz laser may reliably determine lifetime values of ~0.6 ns, but not lifetime values in the ps range. Thus, even if additional lifetime components in the ps time range do exist, they cannot be detected using the present system. For example, it has been suggested, based on molecular dynamics calculations, that the rotation time for the indole ring is in the range of 2–20 ps (Lakowicz and Gryczynski, 1991). If true, detection of this motion requires a modulation of intensity up to 2 GHz (Lakowicz and Gryczynski, 1991). These shortcomings aside, our present data warranted further investigation into the dynamics and thermodynamics of complex interactions involved in the regulation of *E. coli* PFK. Perhaps the implications of the heightened sensitivity of the position-55 tryptophan-shifted fluorophore can be tested using a more recent setup, which allows for modulation of intensity up to 2 GHz.

This work was performed by A.S.P. at Texas A&M University in partial fulfillment of the dissertation for a Ph.D. in Biochemistry.

A.S.P. was a recipient of the Patricia Roberts Harris Fellowship. This work was supported by grant GM33216, to G.D.R., from the National Institutes of Health.

REFERENCES

Alcala, J. R., E. Gratton, and F. G. Prendergast. 1987a. Resolvability of fluorescence lifetime distribution using phase fluorometry. *Biophys. J.* 51:587–596.

Alcala, J. R., E. Gratton, and F. G. Prendergast. 1987b. Interpretation of fluorescence decays in proteins using continuous lifetime distributions. *Biophys. J.* 51:925–936.

Ansari, A., J. Berendzen, S. F. Bowne, H. Frauenfelder, I. E. T. Iben, T. B. Sauke, E. Shyamunder, and R. D. Young.1985. Protein states and protein quakes. *Proc. Natl. Acad. Sci. USA.* 82:5000–5004.

Auzat, I., G. Le Bras, P. Branny, F. De La Torre, B. Theunissen, and J. R. Garel. 1994. The role of Glu187 in the regulation of phosphofructokinase by phosphoenolpyruvate. *J. Mol. Biol.* 235:68–72.

Beechem, J. M., E. Gratton, M. Ameloot, J. R. Knutson, and L. Brand. 1991. Global analysis of fluorescence intensity and anisotropy decay data: second-generation theory and programs. *In* Topics in Fluorescence Spectroscopy, Vol 2: Principles. J.R. Lakowicz, editor. Plenum Press, New York. pp.241–303.

Blangy, D., H. Buc, and J. Monod. 1968. Kinetics of the allosteric interactions of phosphofructokinase from *Escherichia coli*. *J. Mol. Biol.* 31:13–35.

Braxton, B. L., L. S. Mullins, F. M. Raushel, and G. D. Reinhart. 1996. Allosteric effects of carbamoyl phosphate synthetase from *Escherichia coli* are entropy-driven. *Biochemistry.* 35:11918–11924.

Callis, P. R. 1999. Origin of nonexponential tryptophan fluorescence decay in proteins. Presented at the Biophysical Society 43rd Annual Meeting, Baltimore, MD.

Daugherty, M. A., M. A. Shea, J. A. Johnson, V. J. Licata, G. J. Turner, and G. K. Ackers. 1991. Identification of the intermediate allosteric species in human hemoglobin reveals a molecular code for cooperative switching. *Proc. Natl. Acad. Sci. USA.* 88:1110–1114.

Demchenko, A. P. 1994. Protein fluorescence, dynamics and function: exploration of analogy between electronically excited and biocatalytic transition states. *Biochim. Biophys. Acta.* 1209:149–164.

Gratton, E., J. R. Alcala, and G. Marriott. 1986. Rotations of tryptophan residues in proteins. *Biochem. Soc. Trans.* 14:835–838.

Gratton, E., and M. Limkeman. 1983. Resolution of mixtures of fluorophores using variable-frequency phase and modulation data. *Biophys. J.* 44:315–324.

Gratton, E., M. Limkeman, J. R. Lakowicz, B. P. Maliwal, H. Cherek, and G. Laczko. 1984. Resolution of mixtures of fluorophores using variable-frequency phase and modulation data. *Biophys. J.* 46:479–486.

Haran, G., E. Haas, B. K. Szpikowska, and M. T. Mas. 1992. Domain motions in phosphoglycerate kinase: determination of interdomain distance distributions by site-specific labeling and time-resolved fluorescence energy transfer. *Proc. Natl. Acad. Sci. USA.* 89:11764–11768.

Jameson, D. M., E. Gratton, and R. D. Hall. 1984. Measurement and analysis of heterogeneous emissions by multifrequency phase and modulation fluorometry. *Appl. Spectrosc. Rev.* 20:55–106.

Jameson, D. M., and T. L. Hazlett. 1991. Time-resolved fluorescence in biology and biochemistry. *In* Biophysical and Biochemical Aspect of Fluorescence Spectroscopy. T.G. Dewey, editor. Plenum Press, New York. pp.105–133.

Jameson, D. M., and W. H. Sawyer. 1995. Fluorescence anisotropy applied to biomolecular interactions. *Methods Enzymol.* 246:283–300.

Johnson, M. 1997. Multiple-domain fluorescence lifetime data analysis. *Methods Enzymol.* 278:570–583.

Johnson, J. L., and G. D. Reinhart. 1994. Influence of MgADP on phosphofructokinase from *Escherichia coli*. Elucidation of coupling interactions with both substrates. *Biochemistry.* 33:2635–2643.

Johnson, J. L., and G. D. Reinhart. 1997. Failure of a two-state model to describe the influence of phospho(enol)pyruvate on phosphofructokinase from *Escherichia coli*. *Biochemistry.* 36:12814–12822.

Knutson, J. R. 1992. Alternatives to consider in fluorescence decay analysis. *Methods Enzymol.* 210:357–373.

Knutson, J. R., L. Davenport, and L. Brand. 1986. Anisotropy decay associated fluorescence spectra and analysis of rotational heterogeneity. 1. Theory and applications. *Biochemistry.* 25:1805–1810.

Lakowicz, J. 1983. Fluorescence polarization. *In* Principle of Fluorescence. Plenum Press, New York. pp.112–150.

Lakowicz, J. R., H. Cherek, and A. Balter. 1981. Correction of timing error in photomultiplier tubes used in phase-modulation fluorometry. *J. Biochem. Biophys. Metab.* 5:131–146.

Lakowicz, J. R., and I. Grycynski. 1991. Frequency domain in fluorescence spectroscopy. *In* Topics in Fluorescence Spectroscopy, Vol. 1: Techniques. J.R. Lakowicz, editor. Plenum Press, New York. pp.293–335.

Lakowicz, J. R., G. Laczko, H. Cherek, E. Gratton, and M. Limkeman. 1984. Analysis of fluorescence decay kinetics from variable-frequency phase shift and modulation data. *Biophys. J.* 46:463–477.

Lau, F. T.-K., and A. R. Fersht. 1987. Conversion of allosteric inhibition to activation in phosphofructokinase by protein engineering. *Nature.* 326:811–812.

Lau, F. T.-K., and A. R. Fersht. 1989. Dissection of the effector-binding site and complementation studies of *Escherichia coli* phosphofructokinase using site-directed mutagenesis. *Biochemistry.* 28:6841–6847.

Lipari, G., and A. Szabo. 1980. Effects of librational motion on fluorescence depolarization and nuclear magnetic resonance relaxation in macromolecules and membranes. *Biophys. J.* 30:489–506.

Marquardt, D. W. 1963. An algorithm for least-square estimation of nonlinear parameter. *J. Soc. Ind. Appl. Math.* 11:431–441.

Munro, I., I. Pecht, and L. Stryer. 1979. Subnanoseconds motions of tryptophan residues in proteins. *Proc. Natl. Acad. Sci. USA.* 76:56–60.

Pham, T. C. 1999. Thermodynamic, dynamic and kinetic characterization of the E187A mutant of *Escherichia coli* phosphofructokinase. Dissertation. Texas A and M University.

Pham, A. S., F. Janiak-Spens, and G. D. Reinhart. 2001. Persistent binding of MgADP to the E187A mutant of *Escherichia coli* phosphofructokinase in the absence of allosteric effects. *Biochemistry.* 40:4140–4149.

Pham, A. S., and G. D. Reinhart. 2001a. MgATP-dependent activation by phosphoenolpyruvate of the E187A mutant of *Escherichia coli* phosphofructokinase. *Biochemistry.* 40:4150–4158.

Pham, A. S., and G. D. Reinhart. 2001b. Pre-steady-state quantification of the allosteric influence of *Escherichia coli* phosphofructokinase. *J. Biol. Chem.* 267:34388–34395.

Platt, J. R. 1951. Isoconjugate spectra and variconjugate sequences. *J. Chem. Phys.* 19:101–104.

Shirakihara, Y., and P. R. Evans. 1988. Crystal structure of the complex of phosphofructokinase from *Escherichia coli* with its reaction products. *J. Mol. Biol.* 204:973–994.

Spencer, R. D., and G. Weber. 1969. Measurements of subnanosecond fluorescence lifetimes with a cross-correlation phase fluorometer. *Ann. N. Y. Acad. Sci.* 158:361–376.

Szmacinski, H., R. Jayaweera, H. Cherek, and J. R. Lakowicz. 1987. Demonstration of an associated anisotropy decay by frequency-domain fluorometry. *Biophys. Chem.* 27:233–241.

Tlapak-Simmons, V., and G. D. Reinhart. 1994. Comparison of the inhibition by phospho(enol)pyruvate and phosphoglycolate of phosphofructokinase from *B. stearothermophilus*. *Arch. Biochem. Biophys.* 308:226–230.

Valeur, B., and G. Weber. 1977. Resolution of the fluorescence excitation spectrum of indole into the 1La and 1Lb excitation bands. *Photochem. Photobiol.* 25:441–444.

Wells, J. A. 1990. Additivity of mutational effects in proteins. *Biochemistry.* 29:8509–8517.